

# In vivo measurement of cytoplasmic organelle water fraction using diffusion-weighted imaging

## Application in the malignant grading and differential diagnosis of gliomas

Chenhan Ling, MD<sup>a</sup>, Feina Shi, MD<sup>b</sup>, Jianmin Zhang, MD, PhD<sup>a</sup>, Biao Jiang, MD<sup>c</sup>, Fei Dong, MD<sup>c</sup>, Qiang Zeng, MD<sup>a,\*</sup>

### Abstract

Recently, we have proposed a theoretical modified tri-exponential model for multi-b-value diffusion-weighted imaging (DWI) to measure the cytoplasmic organelle water fraction (COWF). This study aims to investigate whether COWF maps are effective in evaluating the malignant degree of gliomas and distinguishing primary central nervous system lymphomas (PCNSL) from gliomas.

We performed this retrospective study based on our prospectively collected data. All patients underwent preoperative multi-b-value DWI. Parametric maps were derived from multi-b-value DWI maps using the modified tri-exponential model. Receiver operating characteristic analyses were used to assess the diagnostic accuracy of the parameter maps. Pearson correlation coefficients were calculated to investigate the correlations between the parameters and the Ki-67 proliferation index.

A total of 66 patients were enrolled, including 16 low-grade gliomas (LGG), 45 high-grade gliomas (HGG), and 5 PCNSL. The mean COWF values were significantly different among LGG ( $3.1 \pm 1.4\%$ ), HGG ( $6.9 \pm 2.8\%$ ), and PCNSL ( $14.0 \pm 2.2\%$ ) ( $P < .001$ ). The areas under the curves of the mean COWF value in distinguishing HGG from LGG and distinguishing PCNSL from gliomas were 0.899 and 0.980, respectively. The mean COWF value had a moderate correlation with the Ki-67 proliferation index ( $r=0.647$ ).

The COWF map is useful in malignant grading of gliomas, and may be helpful in distinguishing PCNSL from gliomas.

**Abbreviations:** AUC = area under the curve, COWF = cytoplasmic organelle water fraction, DWI = diffusion-weighted imaging, HGG = high-grade gliomas, LGG = low-grade gliomas, PCNSL = primary central nervous system lymphomas, ROC = receiver operating characteristic, ROI = regions of interest.

**Keywords:** diffusion magnetic resonance imaging, glioma, Ki-67 antigen, lymphoma, neoplasm grading

## 1. Introduction

Glioma is the most common malignant brain tumor.<sup>[1]</sup> It is of clinical need to classify the grade of gliomas as various stages of gliomas need different therapies. Traditionally, histopathologic

examination is the gold standard for grading gliomas. However, high-grade gliomas (HGG) always contain both low- and high-grade components, leading to sampling error in pathological assessment.<sup>[2,3]</sup> Besides, pathological grading can only achieve after surgery or biopsy, while it would be helpful for neurosurgeons to make individual operation plan if the malignant degrees of different parts of tumors can be identified before surgery. Meanwhile, in clinical practice, there are still difficulties in distinguishing gliomas from some other intracranial tumors, such as primary central nervous system lymphomas (PCNSL). The treatments for PCNSL and gliomas are totally different. Therefore, more precise differential diagnosis of gliomas before surgery can help to avoid unnecessary and costly surgery.

Diffusion-weighted imaging (DWI) is a noninvasive method to evaluate water diffusion in tissues. Several models have been developed to fit multi-b-value DWI, such as stretched-exponential model, bi-exponential model, and kurtosis model. Many studies based on the bi-exponential model have been showed a potential value in grading gliomas and distinguishing PCNSL from gliomas.<sup>[4-6]</sup> However, the bi-exponential model has been challenged for its lack of reproducibility,<sup>[7]</sup> and has been considered as oversimplified.<sup>[8]</sup> Several previous studies have indicated the existence of water molecular pool with extremely low diffusion in tissues.<sup>[9-12]</sup> Recently, we have proposed a theoretical modified tri-exponential model for multi-b-value DWI to measure the cytoplasmic organelle water fraction (COWF).<sup>[13]</sup> COWF means the proportion of water molecules in

Editor: Martin S. Staeger.

CL and FS contributed equally to this work.

This work was support by the National Natural Science Foundation of China (81801654).

The authors have no conflicts of interest to disclose.

<sup>a</sup>Department of Neurosurgery, <sup>b</sup>Department of Neurology, <sup>c</sup>Department of Radiology, Second Affiliated Hospital of Zhejiang University School of Medicine, Hangzhou, Zhejiang, China.

\* Correspondence: Qiang Zeng, Department of Neurosurgery, Second Affiliated Hospital of Zhejiang University School of Medicine, Hangzhou, Zhejiang, 310009, China (e-mail: zengqiang@zju.edu.cn).

Copyright © 2019 the Author(s). Published by Wolters Kluwer Health, Inc. This is an open access article distributed under the terms of the Creative Commons Attribution-Non Commercial License 4.0 (CCBY-NC), where it is permissible to download, share, remix, transform, and buildup the work provided it is properly cited. The work cannot be used commercially without permission from the journal.

How to cite this article: Ling C, Shi F, Zhang J, Jiang B, Dong F, Zeng Q. In vivo measurement of cytoplasmic organelle water fraction using diffusion-weighted imaging. *Medicine* 2019;98:46(e17949).

Received: 28 January 2019 / Received in final form: 31 August 2019 / Accepted: 15 October 2019

<http://dx.doi.org/10.1097/MD.00000000000017949>

the cytoplasmic organelles to the total water molecules in the tissue.

Higher degree of malignancy is always associated with higher cell density in tumors. Besides, swollen cytoplasmic organelles have been detected in highly malignant tumors,<sup>[14,15]</sup> which may be due to vigorous metabolism and relative hypoxia. Hence, COWF may have a positive association with malignant degree of tumors. We performed this preliminary study to investigate the clinical value of the COWF map derived using the modified tri-exponential model in evaluating the malignant degree of gliomas and distinguishing PCNSL from gliomas.

## 2. Materials and methods

### 2.1. Patient selection

This retrospective study was based on our prospectively collected database for consecutive patients with gliomas who were hospitalized at our center between August 2013 and January 2015. This study was approved by the institutional review board of our center. Written informed consents were obtained from all participants. All clinical investigations were conducted according to the principles expressed in the Declaration of Helsinki. This study enrolled patients who

1. underwent a pre-operative MRI examination with a multi-b-value DWI;
2. had a diffusion glioma or PCNSL confirmed by pathologists who were blinded to clinical information.

WHO grade II gliomas are considered as low-grade gliomas (LGG), while WHO grade III and WHO grade IV gliomas are regarded as HGG. The Ki-67 index was examined in 47 glioma patients.

### 2.2. Image data acquisition

The patients were all imaged pre-operatively using a 3.0-T MR system (Discovery MR750, GE Healthcare Systems, Milwaukee, WI) with an 8-channel high-resolution receiver head coil. The DWI sequence was acquired with 9 b-values (0, 100, 200, 300, 500, 700, 1000, 2000, and 3000 s/mm<sup>2</sup>) in three orthogonal directions using a single-shot echo planer imaging with the following parameters: repetition time/echo time, 3000/88.6 ms; section thickness, 4 mm; spacing between slices, 5 mm; field of view, 240 × 240 mm; matrix, 256 × 256; phase FOV, 1.00; flip angle, 90; and pixel bandwidth, 1953.1 Hz/pixel. The number of scan averages varied from one for b=0 s/mm<sup>2</sup> to six for b=3000 s/mm<sup>2</sup>. The scan time of the DWI sequence was 3 min 6 s. In addition, a contrast-enhanced T2-flair sequence was also performed with the same sections after the injection of gadodiamide (Omniscan, Nycomed Imaging, Oslo, Norway) with a dose of 10 mL.

### 2.3. Model

The modified tri-exponential mode contains three compartments: the strictly diffusion-limited compartment, slow diffusion compartment, and fast diffusion compartment. Theoretically, the strictly diffusion-limited compartment represents water molecules strictly limited in cytoplasmic organelles with extremely small space, and the slow diffusion compartment represents water molecules in cytoplasmic matrix and cell

nucleus, while the fast diffusion compartment represents extracellular water molecules.<sup>[13]</sup> The equation of the modified tri-exponential model is expressed as follows:

$$\frac{S}{S_0} = f_0 + f_{slow} * e^{-ADC_{slow} * b} + f_{fast} * e^{-ADC_{fast} * b}, f_0 + f_{slow} + f_{fast} = 1 \quad (1)$$

where  $S$  represents the signal intensity at corresponding  $b$ , and  $S_0$  represents the signal intensity at  $b=0$  s/mm<sup>2</sup>, and  $f_0$ ,  $f_{slow}$ , and  $f_{fast}$  represent the fractions of the strictly diffusion-limited compartment, slow diffusion compartment and fast diffusion compartment, respectively. Here, we termed  $f_0$  map as COWF map.

### 2.4. Image processing and analysis

Parametric maps were generated using the method described detailed in a previous study.<sup>[13]</sup> The regions of interest (ROI) were volumetric, manually placed slice by slice on the DWI images with  $b=3000$  s/mm<sup>2</sup> by an experienced neuroradiologist with 20 years' experience who was blinded to patients' clinical information. The solid tumor areas were included in the ROIs as many as possible, while the regions of necrosis, cystic lesions and hematoma were excluded carefully. Then, the ROIs were copied to the parameter maps, and the mean COWF,  $f_{slow}$ ,  $f_{fast}$ ,  $ADC_{slow}$ , and  $ADC_{fast}$  values were calculated for each ROI. In addition, ROIs were also drawn by a junior neurosurgeon, and the mean values of the parameters were calculated in order to assess the interobserver concordance.

### 2.5. Statistical analysis

All statistical analyses were performed with SPSS version 22 (IBM, Armonk, New York, NY). The intraclass correlation coefficient was used to assess interobserver concordance for the measurement of the parameters. KS normality test was used to test whether the parameters obey normal distribution. One-way ANOVA followed by LSD test was used to compare difference among three groups. Receiver operating characteristic (ROC) curves were generated for parameters in differentiating HGG from LGG and differentiating PCNSL from gliomas. The area under the curve (AUC), sensitivity, specificity, and best cut-off value were determined for each parameter. Pearson correlation analysis was performed to investigate the correlations between the parameters and the Ki-67 index. A value of  $P < .05$  was regarded as statistically significant.

## 3. Results

### 3.1. Patient characteristics

A total of 66 patients (females, 28 [41.2%]; age, 50 ± 21 years) were enrolled, including 61 gliomas (females, 27 [44.2%]; age, 49 ± 21 years) and 5 PCNSL (female, 1 [20%]; age, 60 ± 12 years). Among these gliomas, there were 16 LGG and 45 HGG (WHO grade II, 16; WHO grade III, 17; WHO grade IV, 28).

### 3.2. Interobserver concordance

Manifestations of LGG, HGG, and PCNSL in parametric maps generated using the modified tri-exponential model are shown in Figure 1. The intraclass correlation coefficients for the measurements of the mean COWF,  $f_{slow}$ ,  $f_{fast}$ ,  $ADC_{slow}$  and

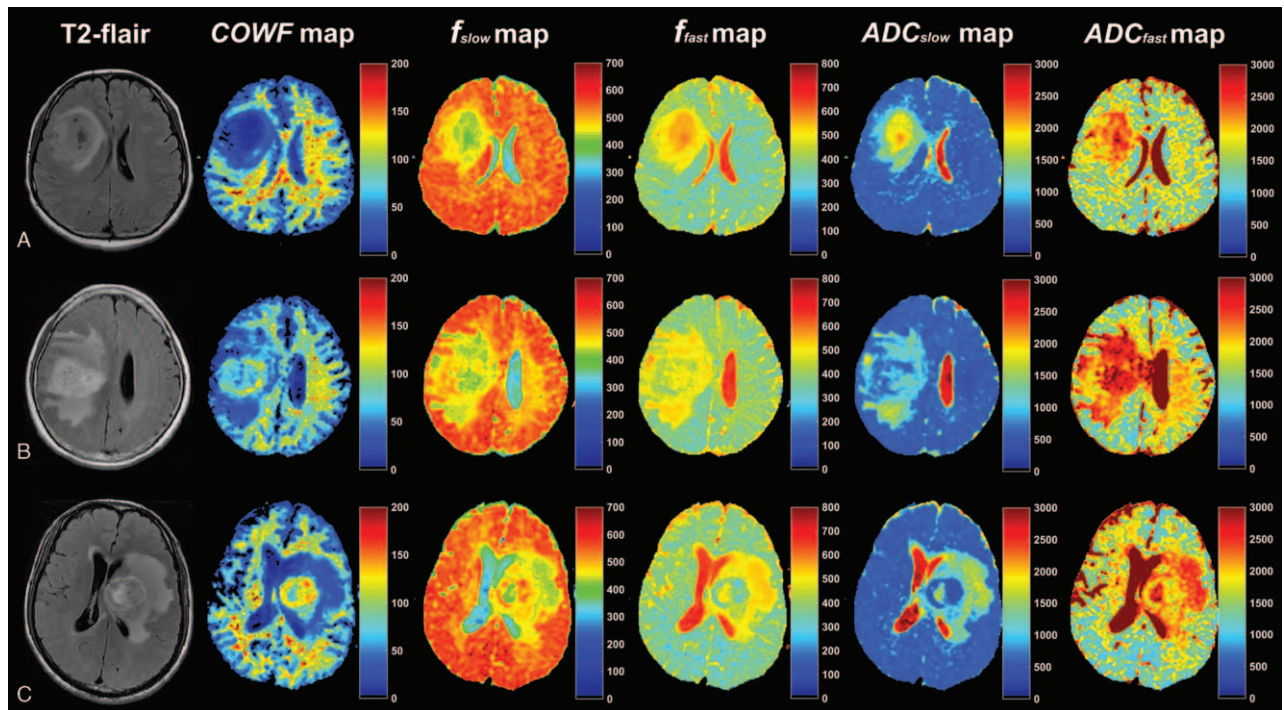


**Figure 1.** Illustrations of a 32-year-old female with astrocytoma (WHO grade II) (A), a 68-year-old female with anaplastic astrocytoma (WHO grade III) (B), and a 45-year-old male with primary central nervous system lymphoma (C). The contrast-enhanced T2-flair maps, COWF maps,  $f_{slow}$  maps,  $f_{fast}$  maps,  $ADC_{slow}$  maps, and  $ADC_{fast}$  maps are shown in first to sixth rows, respectively. The unit for the COWF and  $f$  maps is %, and the unit for ADC maps is  $\times 10^{-6} \text{mm}^2/\text{s}$ .

$ADC_{fast}$  values were 0.944, 0.843, 0.899, 0.875, and 0.863, respectively.

### 3.3. Parameters in each tumor group

Figure 2 shows the box plots of parameters of different grades of gliomas and PCNSL. The COWF value had an obviously increasing tendency with the grade of gliomas, while  $f_{fast}$  and  $ADC_{slow}$  had decreasing tendencies. There was no significant difference in  $ADC_{fast}$  between any pairs of subgroups. The mean COWF values were significantly different among LGG ( $3.1\% \pm 1.4\%$ ), HGG ( $6.9\% \pm 2.8\%$ ), and PCNSL ( $14.0\% \pm 2.2\%$ ) ( $P < .001$ ), shown in Table 1. The mean COWF value was significantly higher in PCNSL than in HGG ( $P < .001$ ), and also significantly higher in HGG than in LGG ( $P < .001$ ). On the contrary, the mean  $f_{fast}$  value was significantly lower in PCNSL than in HGG ( $P < .001$ ), and also significantly lower in HGG than in LGG ( $P < .001$ ). When compared with LGG, PCNSL, and HGG had significantly higher mean  $f_{slow}$  value ( $P = .032$  and  $.042$ , respectively) and significantly lower mean  $ADC_{slow}$  value (both  $P < .001$ ). There was no significant difference in the mean  $ADC_{fast}$  value among LGG, HGG, and PCNSL.

### 3.4. ROC analysis

The ROC curves of parameters in distinguishing HGG from LGG and in distinguishing PCNSL from gliomas are shown in Figure 3. The AUC, cutoff value, sensitivity and specificity of the mean COWF value were 0.899, 4.0%, 84.4%, and 81.3%, respectively, in distinguishing HGG from LGG; and they were 0.980, 12.1%, 100%, and 96.7%, respectively, in distinguishing PCNSL from gliomas (Table 2). The AUC of the mean  $f_{slow}$ ,

$f_{fast}$ , and  $ADC_{slow}$  values were 0.704, 0.820, and 0.798, respectively, in distinguishing HGG from LGG; and were 0.646, 0.941, and 0.839, respectively, in distinguishing PCNSL from gliomas.

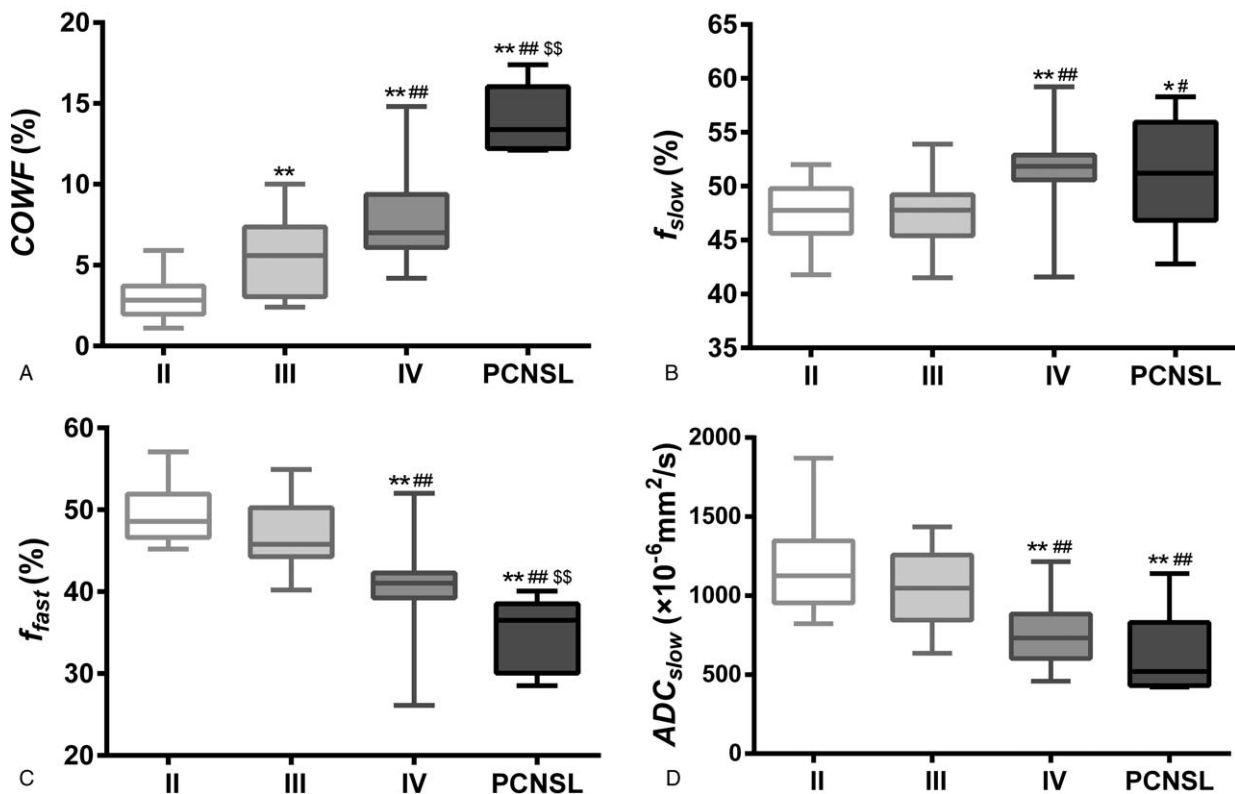
### 3.5. Correlation with the Ki-67 index

Figure 4 demonstrates the correlations between the mean parameter values and the Ki-67 index. The mean COWF value had a moderate correlation with the Ki-67 index ( $r = 0.647$ ,  $P < .001$ ). Meanwhile, the mean  $f_{slow}$  value ( $r = 0.421$ ,  $P = .003$ ),  $f_{fast}$  value ( $r = -0.583$ ,  $P < .001$ ),  $ADC_{slow}$  value ( $r = -0.476$ ,  $P < .001$ ) showed mild correlations with the Ki-67 index. There were no significant association between the mean  $ADC_{fast}$  value and the Ki-67 index ( $P = .201$ ).

## 4. Discussion

In the present study, four parametric maps (COWF,  $f_{slow}$ ,  $f_{fast}$ ,  $ADC_{slow}$ ) derived using the new model were found to be effective in grading gliomas and distinguishing PCNSL from gliomas. Besides, these parameters also showed significant correlations with the Ki-67 index. The COWF, a new parameter representing cytoplasmic organelle water fraction, showed the highest clinical value among all the parameters of the model. Particularly, when compared with the  $ADC_{1000}$  and  $ADC_{3000}$  maps as previously reported,<sup>[16]</sup> the COWF map was found to be more useful in evaluating the grade and proliferation activity of gliomas.

In the present study, we found that the COWF value dramatically increased with the grade of gliomas. In gliomas, the swelling mitochondria and dilated cisterns of endoplasmic reticulum have been detected by previous studies.<sup>[14,15]</sup> Besides,



**Figure 2.** The box plots of the mean COWF (A),  $f_{slow}$  (B),  $f_{fast}$  (C), and  $ADC_{slow}$  (D) values in different grades of gliomas and primary central nervous system lymphomas (PCNSL). \* $P < .05$ , \*\* $P < .01$  compared with grade II gliomas; # $P < .05$ , ## $P < .01$  compared with grade III gliomas; \$\$ $P < .01$  compared with grade IV gliomas.

significant differences in microstructure have been spotted out among different malignant degrees of gliomas.<sup>[17]</sup> Other microstructure changes including swollen mitochondria, distended Golgi complex, and distended endoplasmic reticulum have been detected in glioblastomas.<sup>[18,19]</sup> As for PCNSL, polysomes, and rough endoplasmic reticulum were found to be abundant in lymphoblastomas.<sup>[20]</sup> Accordingly, the fraction of water molecules strictly limited in cytoplasmic organelles may increase and become a significant compartment in high-malignant tumors.

According to previous studies, minimum ADC value derived by the mono-exponential model was smaller in HGG than in

LGG.<sup>[21,22]</sup> Previous studies have also shown that lower ADC value correlated well with higher cellularity.<sup>[23,24]</sup> The hypothesis proposed in previous studies is that tumor tissue with high cellularity decreases in extracellular space resulting in a decreased ADC value.<sup>[21,25]</sup> HGG has higher cellularity than LGG, while PCNSL has even higher cellularity than gliomas.<sup>[21,25,26]</sup> In the present study, the  $f_{fast}$  value, which represents the volume fraction of extracellular space, decreased with the grade of gliomas increasing, and was even lower in PCNSL than in gliomas. These findings in the present study are consistent with the facts that the extra-cellular space is smaller in PCNSL than in HGG and also smaller in HGG than in LGG, demonstrating that the new model may reveal more detailed microstructure characters of tumor tissues.

Previous studies have also found that ADC had a correlation to Ki-67 index.<sup>[27]</sup> In the present study, four parameters derived by the modified tri-exponential model also showed significant correlations with the Ki-67 index. Although ADC value was negatively correlated with cellularity and proliferation index, Rose et al found there was a weak correlation between minimum ADC area and the high FDOPA uptaking area of HGG, suggesting that tissue compression or ischemia may contribute to the restricted diffusion.<sup>[28]</sup> In our view, hypo-vascular tumor tissues of HGG may lead to cytoplasmic organelles swelling due to hypoxia. Thus, fraction of the strictly diffusion-limited compartment may increase in the hypoxic areas, leading to a low ADC value.

Recently, as 3.0 T MR systems being increasingly available, high b-value DWI has been applied more frequently. Several

**Table 1**  
Measurements of parameters derived by the modified tri-exponential model in LGG, HGG and PCNSL.

Parameters	LGG	HGG	PCNSL
COWF (%)	3.1 ± 1.4	6.9 ± 2.8***	14.0 ± 2.2***,###
$f_{slow}$ (%)	47.6 ± 2.8	49.8 ± 3.6*	51.4 ± 5.6*
$f_{fast}$ (%)	49.3 ± 3.4	43.3 ± 5.6***	34.7 ± 4.6***,###
$ADC_{slow}$ ( $\times 10^{-6}$ mm <sup>2</sup> /s)	1178 ± 287	864 ± 257***	609 ± 301***,#
$ADC_{fast}$ ( $\times 10^{-6}$ mm <sup>2</sup> /s)	2045 ± 311	2096 ± 388	1901 ± 206

COWF = cytoplasmic organelle water fraction, HGG = high grade gliomas, LGG = low-grade gliomas, PCNSL = primary central nervous system lymphomas.

\*  $P < .05$ .

\*\*\*  $P < .001$ , compared with LGG.

#  $P < .05$ .

###  $P < .001$ , compared with HGG.

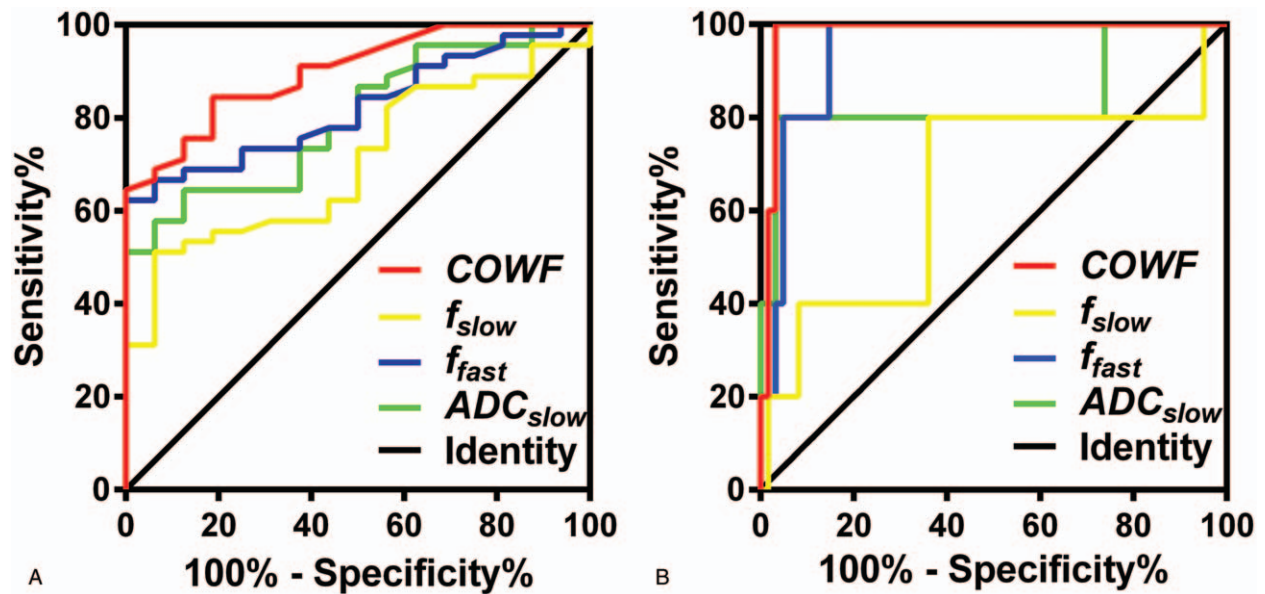


**Figure 3.** Receiver operating characteristic curves of the mean COWF,  $f_{slow}$ ,  $f_{fast}$ , and  $ADC_{slow}$  values in distinguishing high-grade gliomas from low-grade gliomas (A), and distinguishing primary central nervous system lymphomas from gliomas (B).

studies have pointed out that high b-value DWI maps are more valuable in distinguishing the degree of malignancy of tumors.<sup>[16,21,29,30]</sup> However, the potential mechanisms are not clarified. According to the modified tri-exponential model, signal intensity of the strictly diffusion-limited compartment will still remain unchanged at high b-values, while signal intensities of other two compartments will decrease dramatically. As a result, signal intensities on high b-value DWI maps may majorly originate from the strictly diffusion-limited compartment. This might be the reason why high b-value DWI maps are more effective in malignancy grading of tumors than normal b-value DWI maps. As high b-value DWI maps have also been found to be more helpful in several other aspects of tumor evaluation,<sup>[16,31,32]</sup> further researches are needed to investigate the clinical value of the modified tri-exponential model in more aspects of tumor evaluation.

There are several limitations in this preliminary study. First, although the data were prospectively collected, this retrospective study might have a potential risk of selection bias. Second, the

number of PCNSL was small, and this was not persuasive enough for determining the clinical value in distinguishing PCNSL from gliomas. Besides, the diagnostic accuracy of the COWF map in distinguishing HGG from LGG did not verified by a validation group. Further studies enrolling larger samples are needed to verify the diagnostic accuracy of the COWF map in distinguishing PCNSL from gliomas and distinguishing HGG from LGG. Third, this was a retrospective study and the scanning parameters were not optimized. The clinical value of the new model may be further improved after optimizing scanning parameters.

In conclusion, the strictly diffusion-limited compartment is a significant component in PCNSL and HGG. The modified tri-exponential model may provide more detailed information about water diffusion in tumors tissues. The COWF maps derived using the modified tri-exponential model has potential value in preoperative evaluating the grade and proliferation activity of gliomas and distinguishing PCNSL from gliomas. Further studies are needed to verify the clinical value of the COWF maps in tumor evaluations.

**Table 2** Receiver operating characteristic analysis of parameters in distinguishing HGG from LGG and distinguishing PCNSL form gliomas.

Parameters	AUC	Sensitivity (%)	Specificity (%)	Cutoff values
HGG vs LGG				
COWF	0.899	84.4	81.3	4.0
$f_{slow}$	0.704	51.1	93.8	50.8
$f_{fast}$	0.820	62.2	100	45.2
$ADC_{slow}$	0.798	64.4	87.5	926
PCNSL vs gliomas				
COWF	0.980	100	96.7	12.1
$f_{slow}$	0.646	80.0	63.9	50.9
$f_{fast}$	0.941	100	85.3	40.2
$ADC_{slow}$	0.839	80.0	96.7	524.5

The unit of COWF,  $f_{slow}$  and  $f_{fast}$  is %; the unit of  $ADC_{slow}$  is  $\times 10^{-6} \text{mm}^2/\text{s}$ .

AUC=area under the curve, COWF=cytoplasmic organelle water fraction, HGG=high grade gliomas, LGG=low-grade gliomas, PCNSL=primary central nervous system lymphomas.

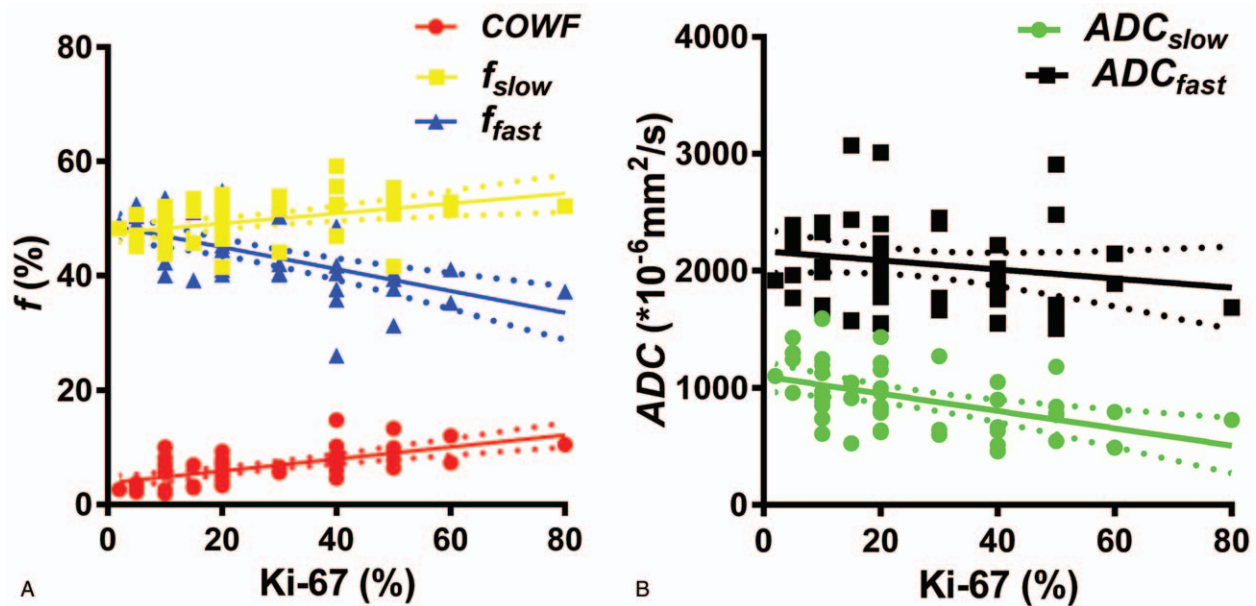


**Figure 4.** The linear regress of the mean  $COWF$ ,  $f_{slow}$ ,  $f_{fast}$  (A) and  $ADC_{slow}$ ,  $ADC_{fast}$  (B) values with the Ki-67 index. Dash lines are the 95% confidence band of the best-fit lines.

## Acknowledgments

This study has received funding by the National Natural Science Foundation of China (grant no. 81801654).

## Author contributions

**Conceptualization:** Jianmin Zhang, Qiang Zeng.  
**Data curation:** Chenhan Ling, Feina Shi, Fei Dong, Qiang Zeng.  
**Funding acquisition:** Qiang Zeng.  
**Investigation:** Jianmin Zhang, Biao Jiang, Qiang Zeng.  
**Methodology:** Chenhan Ling, Feina Shi, Jianmin Zhang, Biao Jiang, Fei Dong, Qiang Zeng.  
**Project administration:** Feina Shi.  
**Software:** Fei Dong.  
**Supervision:** Jianmin Zhang, Biao Jiang.  
**Validation:** Biao Jiang.  
**Visualization:** Biao Jiang.  
**Writing – original draft:** Chenhan Ling, Feina Shi, Fei Dong.  
**Writing – review & editing:** Jianmin Zhang, Qiang Zeng.  
 Qiang Zeng: 0000-0001-6788-067X.  
 Qiang Zeng orcid: 0000-0001-6788-067X.

## References

- [1] Ostrom QT, Gittleman H, Xu J, et al. CBTRUS statistical report: primary brain and other central nervous system tumors diagnosed in the United States in 2009-2013. *Neuro Oncol* 2016;18(suppl\_5):v1-75.
- [2] Prayson RA, Mohan DS, Song P, et al. Clinicopathologic study of forty-four histologically pure supratentorial oligodendrogliomas. *Ann Diagn Pathol* 2000;4:218-27.
- [3] Coons SW, Johnson PC, Pearl DK. The prognostic significance of Ki-67 labeling indices for oligodendrogliomas. *Neurosurgery* 1997;41:878-85.
- [4] Nakajima S, Okada T, Yamamoto A, et al. Primary central nervous system lymphoma and glioblastoma: differentiation using dynamic susceptibility-contrast perfusion-weighted imaging, diffusion-weighted imaging, and 18F-fluorodeoxyglucose positron emission tomography. *Clin Imaging* 2015;39:390-5.
- [5] Shim WH, Kim HS, Choi C-G, et al. Comparison of apparent diffusion coefficient and intravoxel incoherent motion for differentiating among glioblastoma, metastasis, and lymphoma focusing on diffusion-related parameter. *PLoS One* 2015;10:e0134761.
- [6] Bai Y, Lin Y, Tian J, et al. Grading of gliomas by using monoexponential, biexponential, and stretched exponential diffusion-weighted MR imaging and diffusion kurtosis MR imaging. *Radiology* 2016;278:496-504.
- [7] Koh D-M, Collins DJ, Orton MR. Intravoxel incoherent motion in body diffusion-weighted MRI: reality and challenges. *AJR Am J Roentgenol* 2011;196:1351-61.
- [8] Bisdas S, Koh TS, Roder C, et al. Intravoxel incoherent motion diffusion-weighted MR imaging of gliomas: feasibility of the method and initial results. *Neuroradiology* 2013;55:1189-96.
- [9] Sen PN, Basser PJ. A model for diffusion in white matter in the brain. *Biophys J* 2005;89:2927-38.
- [10] Baxter GT, Frank LR. A computational model for diffusion weighted imaging of myelinated white matter. *NeuroImage* 2013;75:204-12.
- [11] Ling X, Zhang Z, Zhao Z, et al. Investigation of apparent diffusion coefficient from ultra-high b-values in Parkinson's disease. *Eur Radiol* 2015;25:2593-600.
- [12] Niendorf T, Dijkhuizen RM, Norris DG, et al. Biexponential diffusion attenuation in various states of brain tissue: implications for diffusion-weighted imaging. *Magn Reson Med* 1996;36:847-57.
- [13] Zeng Q, Shi F, Zhang J, et al. A modified tri-exponential model for multi-b-value diffusion-weighted imaging: a method to detect the strictly diffusion-limited compartment in brain. *Front Neurosci* 2018;12:102.
- [14] Duffell D, Farber L, Chou S, et al. Electron microscopic observations on astrocytomas. *Am J Pathol* 1963;43:539-45.
- [15] Arismendi-Morillo G. Electron microscopy morphology of the mitochondrial network in gliomas and their vascular microenvironment. *Biochim Biophys Acta* 2011;1807:602-8.
- [16] Zeng Q, Dong F, Shi F, et al. Apparent diffusion coefficient maps obtained from high b value diffusion-weighted imaging in the preoperative evaluation of gliomas at 3T: comparison with standard b value diffusion-weighted imaging. *Eur Radiol* 2017;27:5309-15.
- [17] Bergner N, Medyukhina A, Geiger KD, et al. Hyperspectral unmixing of Raman micro-images for assessment of morphological and chemical parameters in non-dried brain tumor specimens. *Anal Bioanal Chem* 2013;405:8719-28.
- [18] Machado CML, Zorzeto TQ, Bianco JER, et al. Ultrastructural characterization of the new NG97ht human-derived glioma cell line using two different electron microscopy technical procedures. *Microsc Res Tech* 2009;72:310-6.

- [19] Arismendi-Morillo GJ, Castellano-Ramirez AV. Ultrastructural mitochondrial pathology in human astrocytic tumors: potentials implications pro-therapeutics strategies. *J Electron Microsc (Tokyo)* 2008;57:33–9.
- [20] Jellinger KA, Paulus W. Primary central nervous system lymphomas—an update. *J Cancer Res Clin Oncol* 1992;119:7–27.
- [21] Kang Y, Choi SH, Kim Y-J, et al. Gliomas: histogram analysis of apparent diffusion coefficient maps with standard- or high-b-value diffusion-weighted MR imaging—correlation with tumor grade. *Radiology* 2011;261:882–90.
- [22] Higano S, Yun X, Kumabe T, et al. Malignant astrocytic tumors: clinical importance of apparent diffusion coefficient in prediction of grade and prognosis. *Radiology* 2006;241:839–46.
- [23] Murakami R, Hirai T, Sugahara T, et al. Grading astrocytic tumors by using apparent diffusion coefficient parameters: superiority of a one-versus two-parameter pilot method. *Radiology* 2009;251:838–45.
- [24] Murakami R, Hirai T, Kitajima M, et al. Magnetic resonance imaging of pilocytic astrocytomas: usefulness of the minimum apparent diffusion coefficient (ADC) value for differentiation from high-grade gliomas. *Acta Radiol* 2009;49:462–7.
- [25] Cha S. Update on brain tumor imaging: from anatomy to physiology. *AJNR Am J Neuroradiol* 2006;27:475–87.
- [26] Guo AC, Cummings TJ, Dash RC, et al. Lymphomas and high-grade astrocytomas: comparison of water diffusibility and histologic characteristics. *Radiology* 2002;224:177–83.
- [27] Fudaba H, Shimomura T, Abe T, et al. Comparison of multiple parameters obtained on 3T pulsed arterial spin-labeling, diffusion tensor imaging, and MRS and the Ki-67 labeling index in evaluating glioma grading. *AJNR Am Neuroradiol* 2014;35:2091–8.
- [28] Rose S, Fay M, Thomas P, et al. Correlation of MRI-derived apparent diffusion coefficients in newly diagnosed gliomas with [18F]-fluoro-L-dopa PET: what are we really measuring with minimum ADC? *AJNR Am Neuroradiol* 2013;34:758–64.
- [29] Hu Y-C, Yan L-F, Sun Q, et al. Comparison between ultra-high and conventional mono b-value DWI for preoperative glioma grading. *Oncotarget* 2017;8:37884–95.
- [30] Seo HS, Chang KH, Na DG, et al. High b-value diffusion ( $b = 3000 \text{ s/mm}^2$ ) MR imaging in cerebral gliomas at 3T: visual and quantitative comparisons with  $b = 1000 \text{ s/mm}^2$ . *AJNR Am Neuroradiol* 2008;29:458–63.
- [31] Chu HH, Choi SH, Ryoo I, et al. Differentiation of true progression from pseudoprogression in glioblastoma treated with radiation therapy and concomitant temozolomide: comparison study of standard and high-b-value diffusion-weighted imaging. *Radiology* 2013;269:831–40.
- [32] Yamasaki F, Kurisu K, Aoki T, et al. Advantages of high b-value diffusion-weighted imaging to diagnose pseudo-responses in patients with recurrent glioma after bevacizumab treatment. *Eur J Radiol* 2012;81:2805–10.